Effect of Time Delay on the Stability of Optoelectronic Oscillators Based on Whispering-Gallery Mode Resonators

Romain Modeste Nguimdo, Virginie Lecocq, Yanne K. Chembo, *Senior Member, IEEE*, and Thomas Erneux

***Abstract*— Optoelectronic oscillators (OEOs) are microwave photonic systems intended to generate ultra-pure radio-frequency signals for aerospace and communication engineering applications. Typically, a long optical fiber delay line is inserted in the feedback loop as an energy storage element intended to improve the phase noise performance. An ultra-high Q whispering-gallery mode resonator can be inserted as well in order to filter-out the spurious ring-cavity peaks arising in the radio-frequency spectrum. However, dynamical instabilities induced by a relatively large delay have never been analyzed for these OEOs. In this paper, we systematically investigate the stability of the generated microwaves as a function of the effective OEO loop gain and delay. We find that close enough to the oscillation threshold, the generated microwaves are unconditionally stable, but as the gain is increased, their stability becomes dependent on the ratio between the time delay and the overall photon lifetime of the resonator. Our results allow an optimal design for these OEOs, leading to both enhanced spectral stability and phase noise performance.**

***Index Terms*— Optoelectronic oscillators, time delay, microwave generation, stability analysis, whispering-gallery mode resonators.**

I. Introduction

OSCILLATORS are devices that produce periodic waves whose amplitude, phase and frequency can be precisely controlled to produce signals that carry information. These devices are an essential element in any system that receives or transmits a signal such as communication systems, radars, sensors, metrology, and other applications where an electromagnetic signal is generated, received or processed. Signals operating with a frequency between 0.3 GHz and 300 GHz (also called microwaves) can be efficiently generated using optoelectronic oscillators (OEOs) [1]–[4]. Most of the microwave applications demand very high spectral purity. To achieve this goal, different energy storage elements have been inserted into the various OEO architectures in order to obtain such microwave sources. The traditional solution is to use long fiber-delay lines (generally up to 4 km of fiber length) inserted into the feedback loop to achieve a high-quality factor [2]–[8]. However, despite their excellent stability performances, these optical delay lines introduce strong spurious ring-cavity peaks at integer multiples of the round-trip frequency [7]. For the reduction or suppression of these peaks, different architectures such as dual-loop configurations [9]–[13], or injection locked systems [14], [15] have been proposed.

Alternatively it has been proposed to replace, in the OEO loop, the fiber delay-line by a whispering-gallery mode resonator (WGMR) with ultra-high Q-factor [1], [16]–[18]. Besides being an efficient technique to circumvent the emergence of the spurious ring-cavity peaks, it also has been demonstrated that the microwaves generated using WGMR-based OEOs are unconditionally stable in the technologically achievable range of parameters [18].

In order to further improve the spectral purity of the microwave sources, we have recently studied an OEO in which a long optical fiber delay line and a WGMR with an ultra-high Q-factor are simultaneously inserted in the feedback loop [19], [20]. Compared to the results for traditional OEOs [2]–[4], [7], [8] and those for WGMR-based OEOs without delay lines [1], [18], OEOs with both a WGMR and a long delay line display a stronger rejection rate for spurious peaks with ultra-low phase noise. However, oscillatory instabilities are possible if the delay is too large [21], [22]. Previous investigations of the WGMR-based OEOs have not considered the time delay in the OEO loop. In real OEO systems, this time delay can vary from few nanoseconds to several tens of microseconds due to the optical fibers connecting the different stand-alone components. It is therefore essential to investigate the stability conditions under which WGMRs and long fiber delay lines can be simultaneously used. Because we are dealing with delay differential equations, such stability analysis is not a routine application of standard linearization techniques.

Our main objective is to determine analytical informations on the stability of a steady output in terms of the gain

Manuscript received July 4, 2016; revised September 23, 2016; accepted September 26, 2016. Date of publication October 10, 2016; date of current version October 21, 2016. The work of R. M. Nguimdo and T. Erneux was supported by FNRS, Belgium. The work of Y. K. Chembo was supported in part by the European Research Council through the Projects StG NextPhase and PoC Versyt, in part by the Centre National d'Etudes Spatiales through the Project SHYRO, in part by Région de Franche-Comté through the Project CORPS, and in part by Labex ACTION. *(Corresponding author: Romain Modeste Nguimdo.)*

R. M. Nguimdo, V. Lecocq, and T. Erneux are with Optique Nonlinéaire Théorique, Université Libre de Bruxelles, 1050 Brussels, Belgium (e-mail: romain.nguimdo@vub.ac.be).

Y. K. Chembo is with the Centre National de la Recherche Scientifique, Département d'Optique, Institut FEMTO-ST, Université Bourgogne-Franche-Comté, 25030 Besançon, France.

Color versions of one or more of the figures in this paper are available online at http://ieeexplore.ieee.org.

Digital Object Identifier 10.1109/JQE.2016.2616129

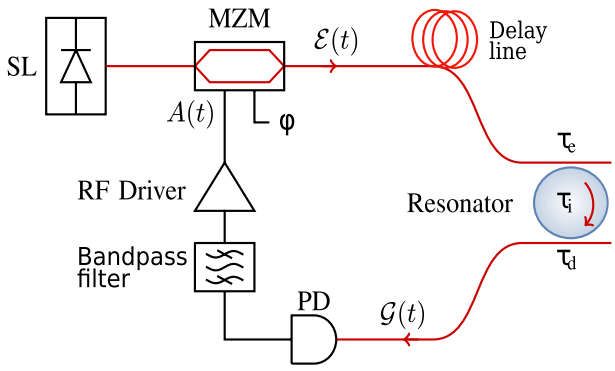

Fig. 1. Experimental setup as used in [18]–[20]. SL: continuous-wave semiconductor laser, MZM: Mach-Zehnder modulator, PD: photodiode. The optical path is in red, while the electric path is in black.

and delay of the feedback loop. Our results will then be substantiated by numerical simulations of the original rate equations.

We first describe the system under study in Sec. II. Then, we derive the model for the microwave envelope in Sec. III. In Sec. IV, we analytically derive the stationary states and investigate their stability while Sec. V is devoted to numerical simulations. Finally, Sec. VII summarizes our main conclusions.

II. The System

The WGMR-based OEO architecture studied in this work has been introduced in [18]–[20]. Its schematic structure is shown in Fig. 1. It is composed of a continuous-wave semiconductor laser which emits a constant power P_0 around 1550 nm. This power seeds a Mach-Zehnder modulator (MZM) having a bias and a radio-frequency (RF) input voltages V_B and $V(t)$, respectively. The RF and the DC half-wave voltages of the MZM are $V_{\pi RF}$ and V_π, respectively. The MZM output signal travels through an optical fiber (with a length which can vary from few meters to several kilometers) before being coupled into a WGMR. Then the WGMR output is subsequently detected by a photodiode and fed into a narrow-band radio-frequency (RF) filter with a central frequency Ω_0 and -3 dB bandwidth $\Delta\Omega$. The output signal of the filter is finally amplified and fed back to the MZM RF electrode to close the loop. In such a system, the effective quality factor Q at the laser wavelength is defined by the intrinsic, excitation (in-coupling) and drop (out-coupling) photon lifetimes τ_i, τ_e and τ_d, respectively. More precisely, $Q = \omega_L \tau$ where $\tau^{-1} = \tau_i^{-1} + \tau_e^{-1} + \tau_d^{-1}$ is the inverse of the overall lifetime of the photon in the resonator and ω_L is the laser frequency. Note that the inverse of τ is the optical bandwidth which defines the OEO filtering.

III. Model

A deterministic model describing the envelope dynamics of the system was introduced in [18]. The relevant variables of the system are the slowly-varying amplitudes of the complex electric field $\mathcal{G}_n(t)$ attached to different WGMR modes, and the microwave amplitude $\mathcal{A}(t) = A(t)e^{i\varphi(t)}$. They satisfy the following equations:

$$\dot{\mathcal{G}}_n = -\left[\frac{1}{\tau} + i\sigma\right]\mathcal{G}_n + \Gamma_n(\phi)\mathrm{J}_n\left(A_T\right)e^{in(\varphi_T - \omega_L T)}, \quad (1)$$

$$\mathcal{A}(t) = 2\beta e^{i\upsilon}\sum_{n=-\infty}^{+\infty}\mathcal{G}_{n+1}\mathcal{G}_n^*, \quad (2)$$

with $A_T \equiv A(t-T)$ and $\varphi_T \equiv \varphi(t-T)$, where T is the overall time delay accumulated during the signal propagation in the optical path (i.e., the time-delay in the optical path from the MZM output to the photodiode without the resonator). J_n is the n^{th}-order Bessel functions of the first kind, n being an integer. υ represents the microwave round-trip phase shift. $\beta = \pi\eta G_0 P_0 S/2V_{\pi\mathrm{RF}}$ is the optoelectronic gain when the effect of the WGMR is not accounted for; G_0, η and S being the amplifier gain, the losses except in the WGMR and the photodetection efficiency, respectively. Note that amplifierless stable oscillations are possible provided sufficient optoelectronic gain. However, amplifiers are more often used to compensate for losses (mainly in the WGMR). $\sigma = \omega_L - \omega_0$ is the detuning frequency between the laser frequency ω_L and the central frequency of the pumped mode ω_0. The term $e^{-in\omega_L T}$ is associated to the static feedback phase introduced by the delay. It can be conveniently set to one as it just shifts the microwave phase $\varphi(t)$. Finally, the term $\Gamma_n(\phi)$ is given by

$$\Gamma_n(\phi) = \frac{1}{\sqrt{\tau_e\tau_d}}\left[e^{i\phi} + (-1)^n e^{-i\phi}\right]i^n, \quad (3)$$

where $\phi = \pi V_B/(2V_\pi)$ is the static phase of the MZM. Note that the dimensionless amplitude $\mathcal{A}(t)$ and the real voltage $V(t)$ are linked by

$$V(t) = \frac{2V_{\pi RF}}{\pi}A(t)\cos\left[\Omega_M t + \varphi(t)\right], \quad (4)$$

where Ω_M is the microwave output angular frequency.

Typically, the dynamics of the system depends on the interplay between the filtering and the feedback terms. When the filtering terms dominate the dynamics, there is no microwave emission (the OEO output shows only noise). When the filtering and the feedback terms interplay equally, pure microwaves are obtained. More complex dynamical behaviours such as modulated microwaves are generated when the feedback terms dominate the dynamics. Our aim is to establish the conditions under which pure microwaves are obtained in OEO systems. Such microwaves are found when the non-trivial fixed point associated with Eqs. (1) and (2) is stable. In the next section, we analyze the linear stability of the non-trivial fixed point.

IV. Non-Trivial Fixed Point and Its Stability

Setting $\dot{\mathcal{G}}_n = 0$ and $\dot{\mathcal{A}} = 0$ and introducing $\mathcal{G}_n = G_n e^{i\Psi_n}$ and $\mathcal{A} = Ae^{i\varphi}$, the non-trivial fixed point of Eqs. (1) and (2) for A is [18]:

$$A^{st} = \frac{1}{2}\mathrm{J}_{\mathrm{c1}}^{-1}\left[\frac{1}{2\Gamma}\right], \quad (5)$$

where $\mathrm{J_{c1}}(x)$ is the Bessel Cardinal function defined as $\mathrm{J_{c1}}(x) = \mathrm{J_1}(x)/x$ and

$$\Gamma = \frac{4\beta\tau^2}{\tau_e\tau_d\left(1+\sigma^2\tau^2\right)}\,|\sin(2\phi)|, \tag{6}$$

is the overall gain satisfying $\Gamma > 1$.

The stability of this non-trivial fixed point can be investigated from the linearized equations. Specifically, we introduce the small perturbations $\delta\mathcal{A}$ and $\delta\mathcal{G}_n$ satisfying $\mathcal{A} = \mathcal{A}^{st} + \delta\mathcal{A}$ and $\mathcal{G}_n = \mathcal{G}_n^{st} + \delta\mathcal{G}_n$ where $|\delta\mathcal{A}| \ll \mathcal{A}^{st}$ and $|\delta\mathcal{G}_n| \ll \mathcal{G}_n^{st}$. From Eqs. (1) and (2), we find:

$$\begin{cases} \delta\dot{\mathcal{A}}_+ = -\left[\dfrac{1}{\tau} + i\sigma\right]\left\{\delta\mathcal{A}_+ - R\left[\delta\mathcal{A}_T + \delta\mathcal{A}_T^*\right]\right\} \\ \delta\dot{\mathcal{A}}_- = -\left[\dfrac{1}{\tau} - i\sigma\right]\left\{\delta\mathcal{A}_- - R\left[\delta\mathcal{A}_T + \delta\mathcal{A}_T^*\right]\right\} \\ \delta\dot{\mathcal{A}}_+^* = -\left[\dfrac{1}{\tau} - i\sigma\right]\left\{\delta\mathcal{A}_+^* - R\left[\delta\mathcal{A}_T + \delta\mathcal{A}_T^*\right]\right\} \\ \delta\dot{\mathcal{A}}_-^* = -\left[\dfrac{1}{\tau} + i\sigma\right]\left\{\delta\mathcal{A}_-^* - R\left[\delta\mathcal{A}_T + \delta\mathcal{A}_T^*\right]\right\}. \end{cases} \tag{7}$$

where $\delta\mathcal{A}_T = \delta\mathcal{A}_+(t-T) + \delta\mathcal{A}_-(t-T)$ with

$$\delta\mathcal{A}_+(t) = 2\beta e^{i\upsilon}\sum_{n=-\infty}^{+\infty}\mathcal{G}_{n-1}^{*st}\delta\mathcal{G}_n, \tag{8}$$

$$\delta\mathcal{A}_-(t) = 2\beta e^{i\upsilon}\sum_{n=-\infty}^{+\infty}\mathcal{G}_{1-n}^{st}\delta\mathcal{G}_{-n}^*. \tag{9}$$

In Eqs. (7), R is given by

$$R = \Gamma\left[\mathrm{J_0}(2A^{st}) - \mathrm{J_2}(2A^{st})\right]/4. \tag{10}$$

The eigenvalues associated with Eq. (7) are typically determined by assuming that the perturbations $\delta\mathcal{A}_+$, $\delta\mathcal{A}_-$, $\delta\mathcal{A}_+^*$ and $\delta\mathcal{A}_-^*$ are proportional to $e^{\lambda t}$, where $\lambda \in \mathbb{C}$. In this case, the stability of the non-trivial fixed point is determined by the determinant of the following block matrix

$$\mathbf{D} = \begin{bmatrix} \mathbf{U} & \mathbf{V} \\ \mathbf{V}^* & \mathbf{U}^* \end{bmatrix}$$

with

$$\mathbf{U} = \begin{bmatrix} \alpha(Re^{-\lambda T} - 1) - \lambda & \alpha Re^{-\lambda T} \\ \alpha^* Re^{-\lambda T} & \alpha^*(Re^{-\lambda T} - 1) - \lambda \end{bmatrix},$$

and

$$\mathbf{V} = \begin{bmatrix} \alpha Re^{-\lambda T} & \alpha Re^{-\lambda T} \\ \alpha^* Re^{-\lambda T} & \alpha^* Re^{-\lambda T} \end{bmatrix},$$

where $\alpha = \tau^{-1} + i\sigma$.

Given the structure of the matrix $\mathbf{D}$, the set of its eigenvalues is the union of the eigenvalues of $\mathbf{U}+\mathbf{V}$ and $\mathbf{U}-\mathbf{V}$. All the real parts of the eigenvalues of $\mathbf{U}-\mathbf{V}$ are negative. Therefore the stability of the system only depends on the sign of the real parts of the eigenvalues of $\mathbf{U}+\mathbf{V}$. These eigenvalues can be obtained from the following characteristic equation

$$\left[\alpha(2Re^{-\lambda T} - 1) - \lambda\right]\left[\alpha^*(2Re^{-\lambda T} - 1) - \lambda\right] - \alpha\alpha^*\left[2Re^{-\lambda T}\right]^2 = 0. \tag{11}$$

Mathematically, the instability occurs at a Hopf bifurcation, i.e, when the real part of λ vanishes. Thus to determine the Hopf bifurcation conditions, we insert $\lambda = i\omega$ into Eq. (11) and separate the real and imaginary parts. We find

$$\begin{cases} \alpha\alpha^*\left[1 - 4R\cos(\omega T)\right] - 2R(\alpha+\alpha^*)\omega\sin(\omega T) - \omega^2 = 0 \\ 4\alpha\alpha^* R\sin(\omega T) + (\alpha+\alpha^*)\omega\left[1 - 2R\cos(\omega T)\right] = 0. \end{cases} \tag{12}$$

Since $\alpha\alpha^* = (1/\tau)^2 + \sigma^2$ and $\alpha + \alpha^* = 2/\tau$, Eqs. (12) can be reformulated as a system of two linear equations with respect to $[1 - 4R\cos(y)]$ and $4R\sin(y)$. They are given by

$$\begin{cases} -4Rz\sin(y) + \left(1+k^2\right)\left[1 - 4R\cos(y)\right] = z^2 \\ \left(1+k^2\right)4R\sin(y) + z\left[1 - 4R\cos(y)\right] = -z \end{cases} \tag{13}$$

where $y = \omega T$, $z = \omega\tau$ and $k = \sigma\tau$. Solving these equations gives

$$\begin{cases} 4R\cos(y) = \dfrac{-k^2z^2 + (1+k^2)^2 + z^2}{(1+k^2)^2 + z^2} \\ 4R\sin(y) = -\dfrac{z(1+k^2+z^2)}{(1+k^2)^2 + z^2}. \end{cases} \tag{14}$$

These equations allow to determine both the Hopf bifurcation points, and the frequency of oscillations at these points. In the next sections, we discuss cases of physical interest depending on the range of values of $k = \sigma\tau$.

A. Case $|k| \ll 1$ or $|\sigma| \ll \tau^{-1}$

The case $k \approx 0$ is of particular interest because, for the WGMR to work properly in the OEO, the laser frequency must be tuned and locked to one of the resonant frequency of the WGMR (i.e $\sigma \approx 0$). In addition, we have demonstrated in our previous works that the phase noise performance degrades with the increase of σ [20]. In practice, the laser frequency and the central frequency of the pumped mode can be matched so that $|\sigma| \ll \tau^{-1}$. In this case, $|k| \ll 1$ implying $1 + k^2 \approx 1$. By solving Eq. (14) with respect to the ratio T/τ and ω, we find

$$\frac{T}{\tau} = \rho_{cr} \tag{15}$$

where

$$\rho_{cr} = \frac{\arccos\left(\dfrac{1}{4R}\right)}{\sqrt{16R^2 - 1}}. \tag{16}$$

Moreover, the angular frequency of the oscillations at this bifurcation point is

$$\omega = \frac{1}{T}\arccos\left(\frac{1}{4R}\right). \tag{17}$$

The fixed point is stable for $\dfrac{T}{\tau} < \rho_{cr}$. This shows that the increase of τ (e.g, the increase of the optical quality factor) or the decrease of the WGMR linewidth (i.e., the inverse of τ) further stabilizes the system. Equations (15) and (17) show that the bifurcation point and the oscillations at this bifurcation point exist if and only if $|R| > 1/4$.

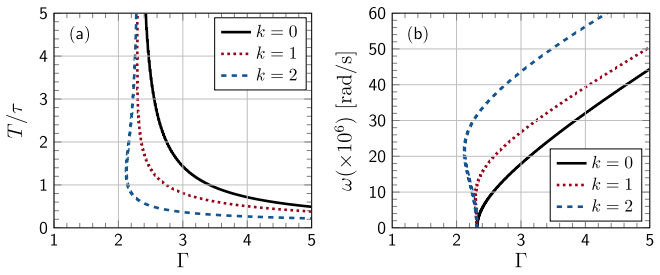

Fig. 2. (a) Necessary and sufficient conditions for asymptotic stability of the trivial solution of Eq. (11). The region below the curve denotes the region in which the microwave amplitudes are stable. (b) Angular frequencies near the bifurcation point for $T = 0.1$ μs.

If $|R| < 1/4$ meaning $\Gamma \leq 2.318$ or $A^{st} \leq 1.2$, the non-trivial fixed point is unconditionally stable. This corresponds to the values of the loop gain for which the filtering and the feedback terms interplay equally independently of the time-delay. A time-delay of any length can therefore be used. If $|R| > 1/4$ meaning $\Gamma > 2.318$, we note from Eq. (15) that the stability of the OEO depends on the ratio between the time delay T and the total lifetime τ of the photon in the resonator. It also depends on the effective OEO loop gain Γ since R is a function of Γ (see Eq. (10)). Figure 2 (a) shows Hopf bifurcation lines in terms of $\rho_{cr} = T/\tau$ and Γ for different values of k. We note that $T < \tau\rho_{cr}$ is always fulfilled for $\Gamma \lesssim 2.318$ implying that the microwaves are unconditionally stable for these values. It means that the delay of any length can be used in this case. For $\Gamma \gtrsim 2.318$ (i.e., $|R| > 1/4$), the time delay T should be chosen so that $T < \tau\rho_{cr}$. In particular, it is found that stable microwaves with an amplitude larger than 1.4 (i.e Γ larger than 3.415) can never be obtained when the delay T is larger than the overall photon lifetime τ. We have found numerically that just before the bifurcation point, the system experiences damped oscillations towards the stable state while such oscillations are sustained just above the bifurcation point. In both cases, the oscillation frequency is the same. Figure 2 (b) shows the angular frequencies of the oscillations at the bifurcation points as a function of the effective overall gain loop. As it can be seen, the oscillation frequency is almost linear with respect to Γ if $k = 0$. Equation (17) also shows that such frequencies are proportional to the inverse of the time delay T.

B. Case $k = O(1)$, i.e., $|\sigma|$ and τ^{-1} Are of the Same Order of Magnitude

Large values of $\sigma = \omega_L - \omega_0$ are obtained when the laser radiation is far away from resonance. More power is therefore needed to pump the WGMR optical mode of interest. This is evidenced in Eq. (6) where it is seen that the increase of $|\sigma|$ is accompanied by the decrease of the overall OEO loop gain. To investigate the influence of σ on the OEO stability, we consider here the case for which $|\sigma|$ and τ^{-1} are of the same order of magnitude.

An analytical expression of the Hopf bifurcation point for any value of k can be obtained from Eq. (14) in parametric form. Specifically, we consider z as a parameter and extract R using Eq. (14):

$$R = -\frac{1}{4}\frac{\sqrt{z^2(1+k^2+z^2)^2 + \left[(1-k^2)z^2 + (1+k^2)^2\right]^2}}{(1+k^2)^2 + z^2}. \tag{18}$$

Using Eq. (14), we obtain y as

$$y = \arccos\left[\frac{1}{4R}\frac{-k^2z^2 + (1+k^2)^2 + z^2}{(1+k^2)^2 + z^2}\right] + 2p\pi \tag{19}$$

where p is an integer. Having y, the ratio T/τ is obtained as y/z.

If $k = 0$, we recover Eq. (15). In general, a family of solutions using different values of the integer p can be obtained for each value of k. We are interested, however, in finding the minimum value of p for which $y > 0$. It gives the first bifurcation responsible for the change of stability of the fixed point.

To illustrate the influence of σ on the OEO stability, we show in Fig. 2 the boundary curve of the stability (a) and the angular frequency near the bifurcation point (b) for $k = 1$ (red) and $k = 2$ (blue). These different curves can be compared with that obtained for $k \approx 0$ shown in the same plot. These two curves indicate that the region of stable microwaves shrinks as $|\sigma|$ increases. For example, if $k = 2$ (i.e $\sigma = 2\tau^{-1}$), the generated microwaves are unstable when $T/\tau > 0.5$ if $\Gamma = 2.5$, while this instability occurs above $T/\tau > 1.5$ for the same Γ when $k = 1$ (i.e $\sigma = \tau^{-1}$). However, the critical value of Γ below which the fixed point is always stable remains almost unchanged for different values of σ. In addition, the influence of σ on the microwave stability is negligible for large values of Γ as all the bifurcation lines in Fig. 2 (a) are coming closer. However, Fig. 2 (b) evidences that the frequency of the oscillations near the bifurcation point significantly changes with $|\sigma|$ for different values of Γ.

V. Numerical Simulations

In order to confirm our analytical predictions, Eqs. (1) and (2) have been numerically integrated using a predictor-corrector method. Different sets of parameter values are possible for a similar system depending on the component characteristics. Here, we use the experimental parameter values in [18]: $V_{\pi\mathrm{RF}} = 4.7$ V, $V_\pi = 4$ V and $V_B = 2$ V, $S = 50\ \Omega \times 0.65$ A/W $= 32.5$ V/W, $P_0 = 20$ dBm, $\sigma = 2\pi \times 159.23$ Hz, $\tau_i = 0.65$ μs, $\tau_e = 2.9$ μs, $\tau_d = 0.1$ μs, $\eta = 8.4$ dB (losses in WGMR and optical fiber). The amplifier gain G_0 is the experimental parameter which can be typical varied and $\eta G_0 P_0$ is the effective power in the microwave loop. These parameters lead to an overall lifetime $\tau = 84.1$ ns corresponding to a Q-factor $Q = 10^8$ for a laser operating at $\lambda = 1552.2$ nm, $\phi = -\pi/4$, $\upsilon = 0$.

The results of the computed bifurcation diagram as a function of the effective loop gain Γ for $T = 0.1$ μs (i.e., 200 m of fiber length) are shown in Fig. 3 (with this value of T, the ratio T/τ is ≈ 1.19). As it can be seen in this figure, stable microwave emissions are obtained for $1 < \Gamma \lesssim 3.19$ (with our considered parameters, this occurs for 30.1 dBm $\leq \eta G_0 P_0 \leq 35.2$ dBm). For $\Gamma \leq 1$

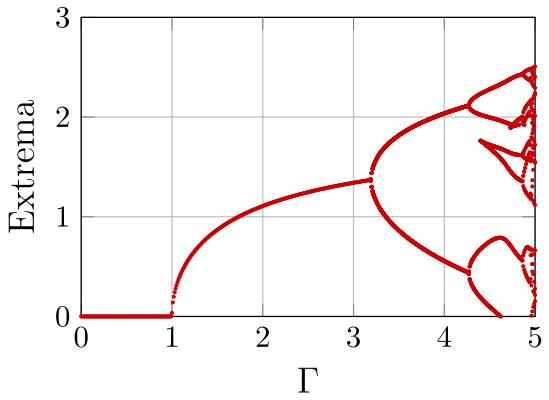

Fig. 3. Numerical bifurcation diagram with respect to Γ for $T = 0.1$ μs. This diagram is obtained by extracting the local extrema from the recorded time series $A(t)$.

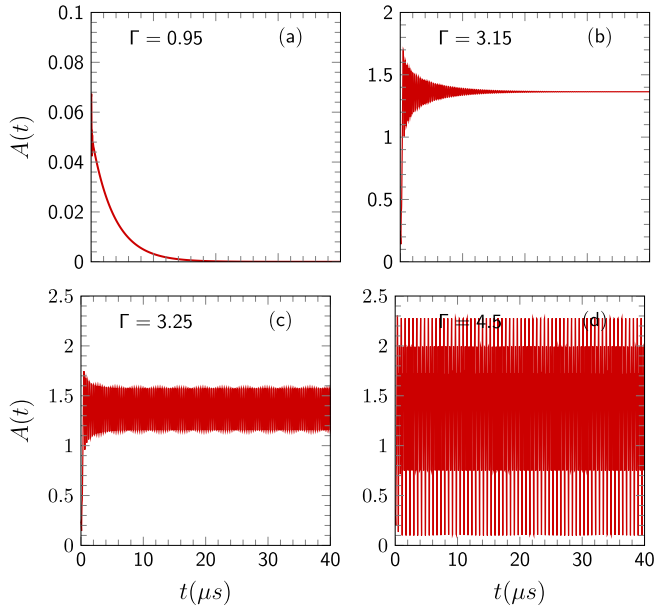

Fig. 4. Numerical simulation of Eqs. (1) and (2) for various gain values when starting with the same initial conditions and considering $T = 0.1$ μs. The transients are displayed to evidence how the OEO dynamics evolves to its stable regime.

(i.e., $\eta G_0 P_0 \leq 30.1$ dBm), there is no microwave emission ($A(t) = 0$ as predicted in [18]). This solution corresponds to zero RF voltage applied to MZM. However, for $\Gamma \gtrsim 3.19$ (i.e., $A(t) \gtrsim 1.369$), the OEO generates complex dynamics. Here, RF voltage applied to MZM is either a multi-periodic signal or a more complex signal which appears to be chaotic. The destabilization of the stationary state from $\Gamma \approx 3.19$ is in excellent agreement with our analytical results in Fig. 2 which predicts that the fixed point loses its stability for a gain higher than $\Gamma = 3.19$ if the ratio $T/\tau > 1.19$. Different types of dynamics are observed depending on Γ. Figure 4 shows some typical envelope dynamics for different values of Γ near the bifurcation points using the same initial conditions. It can be seen that $A(t)$ decays to zero or increases to a nonzero stationary value for $\Gamma = 0.95$ (a) [i.e., $\eta G_0 P_0 = 29.9$ dBm] and $\Gamma = 3.15$ (b) [i.e., $\eta G_0 P_0 = 35.1$ dBm], respectively.

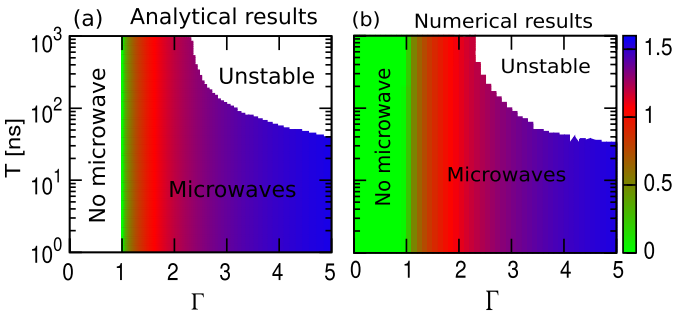

Fig. 5. (a) analytical and (b) numerical results for the microwave amplitudes in the (Γ, T)-plane. The color-scale shows the microwave amplitudes in the stable regions while unstable regions correspond to the modulated amplitudes.

Just below $\Gamma = 3.19$ (i.e., $\eta G_0 P_0 \approx 35.2$ dBm), the system shows damped oscillations [see Fig. 4(b)]. Just above $\Gamma = 3.19$, the oscillations become sustained [see Fig. 4(c)] while keeping the same oscillation frequency (the frequency value of these oscillations is predicted in Fig. 4 (b)).

We next investigate the microwave emission in terms of the time delay T and the loop gain Γ. Figure 5 shows in color scale the microwave amplitudes where they are stable. In (a), the color scale shows the analytically obtained amplitudes if the condition $T < \rho_{cr}$ is satisfied, i.e., the parameter region for which stable microwaves are generated, while in (b) we show the amplitudes when the difference between the extrema in the time series is less than 10^{-5}. In both (a) and (b), we note that if the microwave amplitude is larger than 1.2, the stability strongly depends on the delay size and the overall photon life time.

VI. Discussions

For $k \approx 0$, the above-mentioned threshold of the effective gain for unconditionally stability (i.e., $\Gamma \approx 2.318$) remarkably corresponds to the value above which traditional OEOs based on long optical fibers (i.e the same architecture as here, but without WGMR) have been found to become unstable [6]. In order to investigate an eventual link between the stability of the two architectures, we recall that the deterministic model to describe traditional fiber-based OEOs without resonator is given by [6]:

$$\dot{\mathcal{A}} + \mu \mathcal{A} = \mu \gamma \, \mathrm{J}_1 \left(2A_T\right) e^{i\varphi_T}, \tag{20}$$

where γ is the effective gain and μ is the half-bandwidth of the RF filter in the microwave branch. The variational equation associated to the non-trivial solution of this model is given by

$$\delta\dot{\mathcal{A}} + \mu \delta\mathcal{A} = 2\mu\gamma \, \mathrm{J}_1' \left(2A^{st}\right) \delta\mathcal{A}_T, \tag{21}$$

where prime denotes the derivative of the Bessel function relatively to its argument A^{st}. As $\mathrm{J}_1'(x) = [\mathrm{J}_0(x) - \mathrm{J}_2(x)]/2$, it turns out that characteristic equation for the growth rate is

$$\lambda + \mu \left(1 - 4R' e^{-\lambda T}\right) = 0, \tag{22}$$

where $R' = \gamma \left[J_0(2A^{st}) - J_2(2A^{st})\right]/4$. According to [21], all the real parts of λ are negative if the product $\mu T < \rho'_{cr}$ with

$$\rho'_{cr} = \frac{\arccos\left(\frac{1}{4R'}\right)}{\sqrt{16R'^2 - 1}}. \quad (23)$$

Replacing the inverse of the overall photon lifetime τ^{-1} in Eq. (15) by the half-bandwidth of the RF filter μ, the bifurcation point above which this fiber-based OEO without WGMR becomes unstable is exactly the same as the one for which a WGMR is also inserted in the OEO loop. More concretely, for $k \approx 0$ (i.e., $\sigma \approx 0$), the characteristic equation defining the stability of WGMR-based OEOs [i.e., Eq. (11)] is similar to Eq. (22) which defines the stability of fiber-based OEOs without WGMRs. This shows that, for $\sigma = 0$, the stability of the two architectures can be investigated using the same equation. For example, we note that Eq. (7) reduces to Eq. (21) for $\sigma = 0$.

By solving Eq. (11) for $\sigma = 0$ and Eq. (22), we find that the stability of the two OEO architectures mainly depends on the product of the time delay and the OEO bandwidth. Even for traditional OEOs, the stability boundary condition regarding this product has never been emphasized. In [6], the authors only considered the case for a fixed delay of $T = 20$ μs (i.e., 4 km of fiber length). We would like to mention that in traditional fiber-based OEO architectures, the product μT is typically larger than ρ'_{cr}. Our results therefore explain why stable microwaves have been obtained in these systems only for effective gain values which lead to unconditional stability.

For $k \neq 0$ (i.e., $\sigma \neq 0$), the mathematical model to investigate the linear stability of fiber-based OEOs with WGMR cannot be compared with that used for linear stability analysis of traditional fiber-based OEOs without resonator. The linear stability of fiber-based OEOs with WGMR is investigated from Eq. (7) while that of traditional fiber-based OEOs without resonator is investigated from Eq. (21). The results show that, for any k, the values of the effective loop gains for unconditional stability are almost the same as those found for $k \approx 0$. This means that, for the two OEO architectures, the unconditional stability depends only on the effective gain. However, the boundary stability points differ for the effective loop gains for which the stability depends on the ratio T/τ. This difference is particularly noticeable for the effective gains $2.318 \lesssim \Gamma \lesssim 4$ (i.e., 33.8 dBm$\lesssim \eta G_0 P_0 \lesssim$ 36.1 dBm) where the stability of WGMR-based OEOs strongly depends on the parameter σ [see Fig. 2(a)]. The critical value of T/τ above which microwaves loose their stability becomes smaller with the increase of σ. For $\Gamma \gtrsim 4$, the stability of WGMR-based OEOs still depends on σ, but it is not as significant as in the former case.

VII. Concluding Remarks

We have led a joint analytical and numerical study the effect of time delay on the stability of an OEO based on a WGMR and a delay-line. This stability analysis has allowed us to distinguish between two different ranges of the effective OEO loop gain which can lead to stable microwave generation. For effective OEO loop gain below a given critical value, the generated microwaves are unconditionally stable. Beyond this critical value, the stability of the microwaves strongly depends on the ratio between the time delay and the overall photon lifetime. This stability depends on these three key parameters: the effective overall loop gain, the time delay and the filter bandwidth. Beyond WGMRs, any optical cavity with narrow band can be used for filtering. We expect the same conclusions if a phase modulator is used instead of MZM. Our results are important for the design optimization of these microwave photonics oscillators. It is important to note that large values of the effective gain (i.e., large optical powers) may cause significant nonlinear effects in the WGMR. In the future work, we plan to investigate how the stability of the system depends on the WGMR nonlinearity.

As a final remark, we have noted that, for the effective OEO loop gains leading to unconditional stable fixed points, other types of solutions similar to external cavity modes of a semiconductor laser subject to optical feedback are possible when the laser radiation is far away from resonance. Our preliminary analytical and numerical results indicated that the emergence of such solutions strongly depends on the ratio between the delay and the overall photon lifetime.

References

[1] L. Maleki, "The optoelectronic oscillator," *Nature Photon.*, vol. 5, no. 12, pp. 728–730, 2011.

[2] X. S. Yao and L. Maleki, "High frequency optical subcarrier generator," *Electron. Lett.*, vol. 30, no. 18, pp. 1525–1526, 1994.

[3] X. S. Yao and L. Maleki, "Optoelectronic microwave oscillator," *J. Opt. Soc. Amer. B*, vol. 13, no. 8, pp. 1725–1735, 1996.

[4] X. S. Yao and L. Maleki, "Optoelectronic oscillator for photonic systems," *IEEE J. Quantum Electron.*, vol. 32, no. 7, pp. 1141–1149, Jul. 1996.

[5] Y. K. Chembo, L. Larger, H. Tavernier, R. Bendoula, E. Rubiola, and P. Colet, "Dynamic instabilities of microwaves generated with optoelectronic oscillators," *Opt. Lett.*, vol. 32, no. 17, pp. 2571–2573, 2007.

[6] Y. K. Chembo, L. Larger, and P. Colet, "Nonlinear dynamics and spectral stability of optoelectronic microwave oscillators," *IEEE J. Quantum Electron.*, vol. 44, no. 9, pp. 858–866, Sep. 2008.

[7] Y. K. Chembo, K. Volyanskiy, L. Larger, E. Rubiola, and P. Colet, "Determination of phase noise spectra in optoelectronic microwave oscillators: A langevin approach," *IEEE J. Quantum Electron.*, vol. 45, no. 2, pp. 178–186, Feb. 2009.

[8] Y. K. Chembo, A. Hmima, P.-A. Lacourt, L. Larger, and J. M. Dudley, "Generation of ultralow jitter optical pulses using optoelectronic oscillators with time-lens soliton-assisted compression," *J. Lightw. Technol.*, vol. 27, no. 22, pp. 5160–5167, Nov. 15, 2009.

[9] X. S. Yao, L. Maleki, Y. Ji, G. Lutes, and M. Tu, "A dual-loop opto-electronic oscillator," in *Proc. IEEE Int. Freq. Control. Symp.*, May 1998, pp. 545–549.

[10] L. Maleki, S. Yao, Y. Ji, and V. Ilchenko, "New schemes for improved opto-electronic oscillator," in *Proc. Int. Topical Meeting Microw. Photon.*, vol. 1. 1999, pp. 177–180.

[11] D. Eliyahu and L. Maleki, "Low phase noise and spurious level in multi-loop opto-electronic oscillators," in *Proc. IEEE Int. Freq. Control Symp. PDA Exhibit. Jointly 17th Eur. Freq. Time Forum*, May 2003, pp. 405–410.

[12] J. Yang, Y. Jin-Long, W. Yao-Tian, Z. Li-Tai, and Y. En-Ze, "An optical domain combined dual-loop optoelectronic oscillator," *IEEE Photon. Technol. Lett.*, vol. 19, no. 11, pp. 807–809, Jun. 1, 2007.

[13] R. M. Nguimdo, Y. K. Chembo, P. Colet, and L. Larger, "On the phase noise performance of nonlinear double-loop optoelectronic microwave oscillators," *IEEE J. Quantum Electron.*, vol. 48, no. 11, pp. 1415–1423, Nov. 2012.

[14] E. C. Levy, O. Okusaga, M. Horowitz, C. R. Menyuk, W. Zhou, and G. M. Carter, "Comprehensive computational model of single- and dual-loop optoelectronic oscillators with experimental verification," *Opt. Exp.*, vol. 18, no. 20, pp. 21461–21476, 2010.
[15] O. Okusaga *et al.*, "Spurious mode reduction in dual injection-locked optoelectronic oscillators," *Opt. Exp.*, vol. 19, no. 7, pp. 5839–5854, 2011.
[16] K. Volyanskiy, P. Salzenstein, H. Tavernier, M. Pogurmirskiy, Y. K. Chembo, and L. Larger, "Compact optoelectronic microwave oscillators using ultra-high Q whispering gallery mode disk-resonators and phase modulation," *Opt. Exp.*, vol. 18, no. 21, pp. 22358–22363, 2010.
[17] A. B. Matsko, L. Maleki, A. A. Savchenkov, and V. S. Ilchenko, "Whispering gallery mode based optoelectronic microwave oscillator," *J. Modern Opt.*, vol. 50, nos. 15–17, pp. 2523–2542, 2003.
[18] A. Coillet, R. Henriet, P. Salzenstein, K. P. Huy, L. Larger, and Y. K. Chembo, "Time-domain dynamics and stability analysis of optoelectronic oscillators based on whispering-gallery mode resonators," *IEEE J. Sel. Topics Quantum Electron.*, vol. 19, no. 5, pp. 1–12, Sep./Oct. 2013.
[19] K. Saleh *et al.*, "Phase noise performance comparison between opto-electronic oscillators based on optical delay lines and whispering gallery mode resonators," *Opt. Exp.*, vol. 22, no. 26, pp. 32158–32173, 2014.
[20] R. M. Nguimdo, K. Saleh, A. Coillet, G. Lin, R. Martinenghi, and Y. K. Chembo, "Phase noise performance of optoelectronic oscillators based on Whispering-Gallery mode resonators," *IEEE J. Quantum Electron.*, vol. 51, no. 11, Nov. 2015, Art. no. 6500308.
[21] T. Erneux, *Applied Delay Differential Equations*. New York, NY, USA: Springer, 2009.
[22] T. Erneux and P. Glorieux, *Laser Dynamics*. Cambridge, U.K.: Cambridge Univ. Press, 2010.

Romain Modeste Nguimdo received the M.Sc. degrees in theoretical physics from the University of Dschang, Dschang, Cameroon, and in mechanics from the University of Yaoundé I, Yaoundé, Cameroon, in 2006, and the M.Sc. degree in theoretical physics and the Ph.D. degree from the Instituto de Fsica Interdisciplinary Sistemas Complejos, Palma de Mallorca, Spain, in 2008 and 2011, respectively. From 2012 to 2015, he was a Post-Doctoral Fellow with the Applied Physics Research Group, Vrije Universiteit Brussel, Brussels, Belgium. He is currently an F.N.R.S Fellow with the Université Libre de Bruxelles, Brussels. His current research interests include nonlinear dynamics, optical chaos cryptography, and ultrapure microwaves, random bit generation, and delay-based reservoir computing.

Virginie Lecocq received the master's degree in physics from the Université Libre de Bruxelles in 2013. She is currently the pursuing the Ph.D. degree in laser dynamics with the Optique Nonlinéaire Théorique under the supervision of Prof. T. Erneux. Her master's thesis was on the study of ice rheology. She is a Teaching Assistant in physics with the Solvay Brussels School of Economics and Management.

Yanne K. Chembo (SM'12) received the Ph.D. degree in physics from the University of Yaoundé I in 2005 and the Ph.D. degree in laser physics from the Institute for Cross-Disciplinary Physics and Complex Systems, Palma de Mallorca, Spain, in 2006. In 2007 and 2008, he was a Post-Doctoral Fellow with the Franche-Comté Electronique, Mécanique, Thermique et Optique-Sciences et Technologies Institute, Besançon, France. In 2009, he was a National Aeronautics and Space Administration Post-Doctoral Program Fellow with the Jet Propulsion Laboratory, Pasadena, USA. Since 2010, he has been the Senior Research Scientist with the Center National de la Recherche Scientifique, FEMTO-ST Institute. He has authored over100 articles in international journals and conference proceedings. His research interests involve microwave photonics, optoelectronics, complex systems, and applied nonlinear, stochastic, and quantum dynamics.

Thomas Erneux received the Ph.D. degree in chemistry from the Université Libre de Bruxelles in 1979. After two Post-Doctoral years in the USA, he became a Professor in applied mathematics with Northwestern University from 1982 to 1993. In 1993, he joined the Optique Nonlinéaire Théorique Group, Université Libre de Bruxelles. He is currently the Research Director with the Fonds National de la Recherche Scientifique and a teacher on laser dynamics and asymptotic techniques. Preference is given to collaborative projects with experimental groups and his favorite tools are combinations of numerical and analytical techniques. He has authored two books and over two hundred papers. His current interests concentrate on delay differential equations in all areas of science and, in particular, lasers and nonlinear optics.